Development and characterization of a computer-controlled vidicon spectrometer

ARTICLE *in* ANALYTICAL CHEMISTRY · MARCH 1976

Impact Factor: 5.64 · DOI: 10.1021/ac60367a026

2 AUTHORS, INCLUDING:

Chris Enke
University of New Mexico
198 PUBLICATIONS **4,582** CITATIONS

SEE PROFILE

E. E. Hughes, John Mandel, J. R. McNesby, R. C. Paule, and W. Spangenberg. Special thanks are extended to W. D. Dorko, Analytical Chemistry Division, NBS, for his invaluable assistance in providing propane and oxygen analyses and various gas mixtures.

LITERATURE CITED

(1) J. E. Lovelock, "Gas Chromatography", R. P. W. Scott, Ed., Butterworths, Inc., Washington, D.C., 1960, p 26.
(2) A. Levy, *J. Sci. Instrum.*, **41**, 449 (1964).
(3) Richard Dick and C. Harold Hartman, *Varian Aerograph Tech Bull.* 133-67 (1966).
(4) J. E. Lovelock, *Anal. Chem.*, **33**, 162 (1961).
(5) J. Krugers, "Instrumentation in Gas Chromatography", J. Krugers, Ed., Centrex Publ. Co., Eindhoven, The Netherlands, 1968, p 24.
(6) W. Braun, N. C. Peterson, A. M. Bass, and M. J. Kurylo, *J. Chromatogr.*, **55**, 237 (1971).
(7) H. P. Williams and J. D. Winefordner, *J. Gas Chromatogr.*, **4**, 271 (1966).
(8) G. Greco, Jr., F. Gioia, and F. Alfani, *Chim. Ind.* (*Milan*), **53**, 1133 (1971).
(9) Arthur Fontijon, Alberto Sabadell, and Richard J. Ronco, *Anal. Chem.*, **42**, 575 (1970).
(10) A. Cholette and L. Cloutier, *Can. J. Chem. Eng.*, **37**, 105 (1959).
(11) H. M. McNair and E. J. Bonelli, "Basic Gas Chromatography", 5th ed., Varian Aerograph, Inc., Palo Alto, California, 1969, p 88.
(12) "Gas Chromatography", A. B. Littlewood, Ed., Adlard and Son, Bartholemew Press, Dorking, Surrey, England, 1966, p 431.
(13) J. Mandel, "The Statistical Analysis of Experimental Data", Interscience Publishers, New York, 1964, p 295.
(14) Ref. 13, p 72.
(15) W. Bartok, C. E. Heath, and M. A. Weiss, *AIChE J.*, **6**, 685 (1960).
(16) A. P. Weber, *Chem. Eng. Progr.*, **44**, 26 (1953).
(17) A. P. Weber, *Chem. Eng.*, **76**, 79 (1969).
(18) J. Mandel, Ref. 13, p 118.

RECEIVED for review August 8, 1975. Accepted December 8, 1975. This work was funded in part by the Office of Air and Water Measurement at NBS.

Development and Characterization of a Computer-Controlled Vidicon Spectrometer

T. A. Nieman[1] and C. G. Enke*

Department of Chemistry, Michigan State University, East Lansing, Mich. 48824

A computer-controlled spectrometer using a silicon vidicon multichannel detector has been developed to examine the operating characteristics of imaging devices as spectrometric detectors. Under computer control, the number of electronic channels in the wavelength window can be set between 32 and 4096. The readout beam can be deflected to any channel at random, made to scan them sequentially, or inhibited to increase the target's integration time and enhance weak signals. The system has a single scan *S/N* of 220 which has been extended to 10^4 with signal averaging. *S/N* increases linearly with target integration time up to at least a 20-fold enhancement. The detector responds linearly to the incident light level over at least 3½ orders of magnitude with nonlinear response above 60% of target saturation. With a wavelength window of 230 nm, resolution is about 4 nm with wavelength linearity better than 0.3%. Scan times as fast as 2 ms per frame were used.

The use of multichannel spectrometric detectors employing imaging devices has become widespread. Detectors employing tubes like the silicon vidicon or photodiode arrays have been used for atomic absorption (*1–3*), atomic emission (*4–9*), molecular absorption (*10, 11*), and rapid-scan monitoring of reaction kinetics (*9, 12, 13*) and dc arc processes (*14*). Recently, a pair of articles (*15, 16*) has surveyed the various types of imaging device detectors applicable to spectrometric use. Much of the work by analytical chemists with imaging devices has been with commercial instruments (*2–6*), although some work has been reported with instruments interfaced to a minicomputer for data acquisition and analysis (*1, 7–14*). Despite the growing use of imaging device detectors, it is still difficult for the analytical chemist to gain a clear appreciation of their strengths and weaknesses relative to current detectors.

[1] Present address, School of Chemical Sciences, University of Illinois, Urbana, Ill. 61801.

We wished to gain experience with the use of imaging devices in chemical measurements and to examine the performance characteristics of imaging device detectors. To accomplish this, we have developed a computer-controlled multichannel spectrometer which uses a silicon vidicon tube as the detector. Besides using the computer for data storage and analysis, we have placed the deflection of the readout electron beam under computer control. The computer can position the beam at any wavelength at random, or cause the beam to scan a wavelength region at any of several possible wavelength axis resolutions. In addition, the computer can enable or disable the reading beam to control the target integration time.

This instrument has been used extensively in our laboratory both for conventional spectrometric detection in the visible region and for investigations of reaction kinetics (*17*). Having the instrument under computer control allows the user to easily alter the operating parameters to optimize a particular measurement. This computer control also proved invaluable to studies of the instrument performance characteristics since the computer could cause the instrument to cycle through its combinations of operating parameters with a flexibility not available to hard-wired instruments. In this paper, we wish to report on the design of the instrument and on experiments performed to extend the understanding of how the operating characteristics of imaging devices affect their performance as spectrometric detectors. Future papers will report on chemical applications.

EXPERIMENTAL

A block diagram of the instrument can be seen in Figure 1. The basic units are 1) the power supply, 2) the vidicon tube, deflection assembly, and supporting circuits, 3) the instrument interface, 4) the computer and computer–interface buffer, and 4) the optical path and the dispersion system.

Computer System. The computer around which this system was developed was a Digital Equipment Corporation PDP 8/I minicomputer with 12K words of memory. Standard peripherals

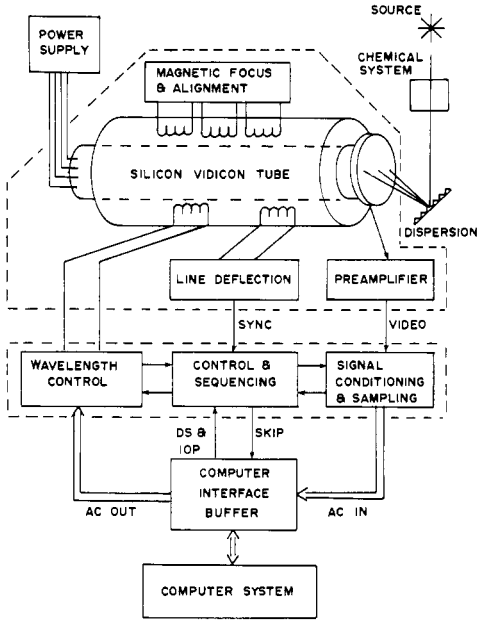

Figure 1. Instrument block diagram

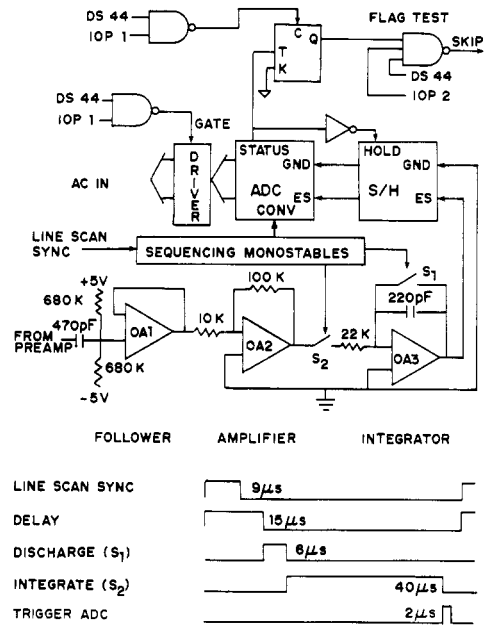

Figure 2. Signal conditioning, sampling, and conversion circuit

included an extended arithmetic element (EAE), dual magnetic tape drives (DECtape), high speed papertape reader and punch, and a KSR35 teletype. In addition, several other peripherals (for alpha-numeric output, data display, and experiment timing) have been interfaced to the 8/I by individuals in our laboratory over the past few years. These have included an RCA 301 lineprinter, a card punch, display controllers for a Varian F-80 X-Y recorder, a Heath EU-205-11 strip chart recorder, and a Tektronix 535A display scope, a character generator for the display scope, and a versatile mainframe real-time clock (*18*). The Heath EU-801E Interfacing System was used for all of the in-house interfacing mentioned above and formed the backbone of the interface for the vidicon spectrometer. Software was developed and run under the OS/8 operating system. Programming was in FORTRAN II with in-line SABR coding for instrument interaction.

Optical Setup. The dispersion system used in the vidicon spectrometer was a modified McPherson EU-700 Czerny-Turner Monochromator. The exit slit was covered, the second folding mirror removed, and the focusing mirror (35 cm) moved forward about 3 cm to cause the focal plane to fall just outside the front of the monochromator housing where the vidicon detector was placed. The original grating with 1180 grooves/mm was replaced by a Bausch and Lomb certified precision grating with 133.6 grooves/mm and blazed at 5461 Å (2°05′). These dispersion optics resulted in a reciprocal linear dispersion of 18 nm/mm in the focal plane. Unless otherwise specified, an entrance slit width of 100 μm and height of 12 mm was used. Since the tube's target is 1.27 cm wide, a 230-nm window is monitored. The vidicon detector is placed in the focal plane of the modified monochromator such that the beam slow-scan axis is parallel to the wavelength axis of the dispersed spectrum. The two-dimensional target is converted into a one-dimensional detector by the wavelength control and the signal conditioning and sampling units. A number of parallel electronic channels are formed on the target, each one at a different wavelength. The information in each wavelength channel is integrated over each fast scan to enhance the signal-to-noise ratio (S/N).

Analog Circuits. The power supply and the tube and deflection assembly support circuits (magnetic focus and alignment, preamplifier, and line deflection are based on conventional television circuitry (*19*). The silicon vidicon tube (RCA 4532), deflection assembly (Cleveland Electronics VYLFA-959), and circuits for magnetic focus and alignment, line deflection, and signal preamplification are contained in a small aluminum box which constitutes the detector. The latter circuits are in close proximity to the tube and deflection assembly because of their high speed and low signal levels. Power for the circuits and for the tube is obtained through shielded cables from the power supply located in a separate box. The line deflection circuit is allowed to run continuously and deflects the beam across a wavelength channel every 65 μs. The video preamplifier is capacitively coupled to the vidicon target. The amplifier is located within 2 cm of the target to which it is connected by a short piece of shielded cable. Target signals of a fraction of a μA are raised to about 100 mV and transmitted on shielded cable to the interface for further conditioning and sampling. The preamplifier has a frequency response of about 4.5 MHz.

The Vidicon Interface. The interface portion of the instrument is contained in an E & L Analog-Digital Designer (ADD) and consists of the circuitry for controlling beam deflection in the wavelength axis, and for conditioning, sampling, and conversion of the video output signal. In addition, the unit contains a data latch, a gated driver, and flags and logic required for transfer of data to and from the computer through the computer interface buffer.

The signal conditioning, sampling, and conversion circuit (Figure 2) receives the video signal from the preamp. The signal is capacitively coupled and biased to just positive of zero volts (the preamp output is biased at −6 V) by summing in signals from the plus and minus five-volt supplies. The +5 V supply is from the ADD: the −5 V supply is obtained from the −15 V ADD supply by using a voltage regulator (National Semiconductor LM304). The signal is then buffered by OA1 and amplified by OA2 (both are type 741 operational amplifiers). The gain of OA2 is normally −10 but can be varied by changing the feedback resistor. Amplifier OA3 (Analog Devices 142B) integrates the video signal as the line deflection circuit samples the target at one wavelength position. Field effect transistor switches S_1 and S_2 control the timing of the integrator for integration and discharge. The signals controlling switches S_1 and S_2 come from a series of four monostable multivibrators which are triggered by the line scan sync signal. This signal occurs every time the line deflection circuit has completed sampling the target at one wavelength and starts to sample at another wavelength. The waveforms for the line scan sync and the outputs of the four monostable multivibrators are shown at the bottom of Figure 2. Integrating the signal produced along a line of diodes in the array detector results in noise reduction (due to averaging out variations in diode sensitivity and dark current) and in signal enhancement. The height of the active region of the target is 9.5 mm, or about 635 diodes (*20*). Although the whole line of diodes is scanned, the signal from only about 400 diodes is integrated (because of timing considerations in the rest of the circuitry). With the specified components and integration time, OA3 has a gain of about −8 but the gain may be adjusted by changing the input resistance. After 40-μs integration time, the ADC (Analog Devices ADC-12QU) is triggered to convert. The ADC status line causes the Sample and Hold (Intronics FS201) to hold during the course of the conversion (15 μs or less) and sets a flag when conversion is complete. When the computer senses the flag, it gates the 12-bit data word into its accumulator and clears the flag.

The basic wavelength deflection (slow scan axis) circuit is diagrammed in Figure 3. This circuit is completely under computer control and produces current in the deflection coil to drive the beam to the wavelength channel of interest. At the heart of the circuit is a 12-bit DAC (Analogic MP1812-2-C high speed 0–+10 volt digital-to-analog converter, slews at 10 V/μs) and a unique preset-

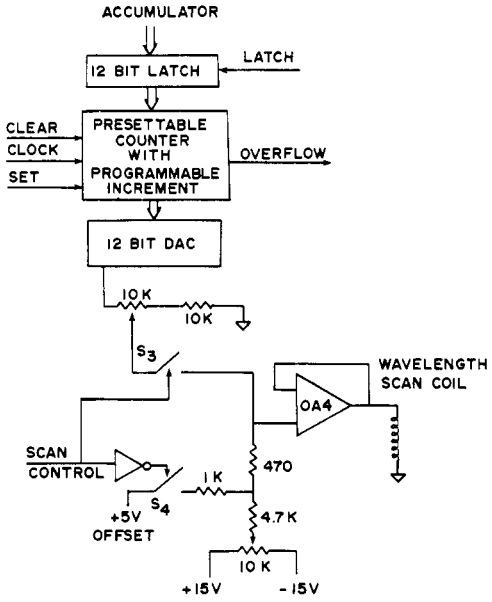

Figure 3. Wavelength deflection circuit

table counter with programmable increment. The 12-bit number in the counter determines the wavelength to which the beam is deflected. The converter's output is buffered by OA4 (Analog Devices 142B) before being applied to the wavelength deflection coil. Since this coil is driven at fairly low frequencies (typically 30–250 Hz), the amplitude of the applied voltage produces an equivalent current amplitude in the coil. Controls are available to adjust the amplitude and centering of the deflection signals and determine whether the target is scanned or allowed to integrate. Closing S_3 allows the DAC to drive the deflection coil. Closing S_4 applies an offset to the coil which drives the beam off the active portion of the target, allowing increased target integration time.

Through the computer software, the wavelength counter allows the user to position the beam at any selected wavelength(s) within the region being monitored or to cause the spectrum to be linearly scanned, and specify the number of wavelength steps into which the spectrum is to be divided. To send the beam to a desired wavelength, the 12-bit word representing that wavelength is loaded into the counter from the computer through the intermediate latch. To cause the spectrum to be scanned, the counter is clocked by the line scan sync, and the word in the data latch controls the magnitude by which the counter increments and so determines the number of channels (in powers of 2 between 32 and 4096) on the wavelength axis. The number of channels into which the axis is divided determines the time required to scan the spectrum. A 64-point spectrum requires 4 ms; a 512-point spectrum requires 33 ms.

The wavelength counter is composed of J–K flip-flops clocked synchronously. By suitable logic controlling, the J and K inputs (Figure 4), the lower bits in the counter can be bypassed depending upon which bit is set in the latch. Each flip-flop can toggle only when either 1) its enable bit is set in the data latch or 2) the Q output and J–K inputs of the previous flip flop are at logical "one". This logic effectively allows the user to change the length of the counter by shifting the position of the least significant bit (lsb). Bits below the lsb are not incremented.

RESULTS AND DISCUSSION

The silicon vidicon spectrometer developed in this research offers great potential to applications which can take advantage of its multichannel and rapid scan capabilities coupled with the processing and control power of an on-line computer. Before proceeding to applications, however, it is necessary to examine the performance characteristics of the instrument. The remainder of this paper describes the experiments undertaken to characterize the operation of the vidicon spectrometer in chemical measurements.

Wavelength Linearity and Resolution. Wavelength scanning in the vidicon spectrometer is accomplished by deflection of an electron beam rather than by a rotating mirror or grating. The linearity of the deflection circuitry

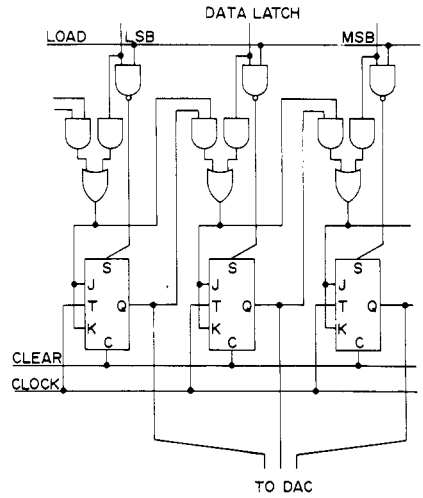

Figure 4. Logic for wavelength counter

Table I. Wavelength Linearity

Spectrum	Channel No.	λ_{true}, nm	$\%(\lambda_{calcd}-\lambda_{true})/\lambda_{true}$
Ho	38	360.8	+0.55
Hg	48	366.3	+0.30
Ho	92	385.8	+0.41
Hg	127	404.6	−0.30
Ho	158	418.5	−0.22
Hg	194	435.8	−0.41
Pr	210	442	−0.16
Ho	217	446	−0.34
Pr	263	467	−0.32
Pr	295	480	+0.02
Ho	422	536.4	+0.32
Hg	442	546.1	+0.20

then determines the linearity of the wavelength axis. Linearity was measured by monitoring the position of lines from the emission spectrum of mercury and from the absorption spectra of a holmium oxide filter and a praseodymium chloride solution. The observed locations of the lines (out of 512 channels), their true wavelengths, and the percentage wavelength error for that channel are listed in Table I. The least squares line through the points has a slope of 0.456 ± 0.003 nm/channel, and the data exhibit a linear correlation coefficient of 0.9997. The average wavelength error is less than 0.3%.

As the electron beam scans across the target on a line scan, it performs an operation equivalent to that of the exit slit of a conventional monochromator, isolating a particular band of wavelengths for observation. Resolution is then determined by the width of the scanning beam. A study concerning resolution examined variation in the observed signal as a function of the number of wavelength channels used to define the spectrum. The 546.1-nm line of the mercury emission spectrum was focused on the target and the height of the peak recorded as the number of wavelength channels was varied from 32 at 4096 by powers of two. The results are shown in Figure 5. Each wavelength channel requires the same amount of time (65 μs) to scan. The exposure time for a channel (T_e) then depends on how many subsequent channels must be scanned before it is rescanned. Since the channel exposure time (T_e) is proportional to the number of channels in the spectrum, one might expect the observed signal to steadily increase as the number of wavelength channels is increased. Instead, the response increases to a plateau and then decreases. This behavior is observed because the "effective" area (or num-

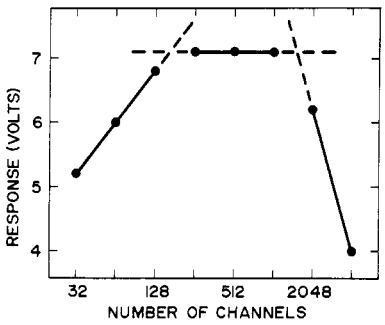

Figure 5. Response vs. number of wavelength channels

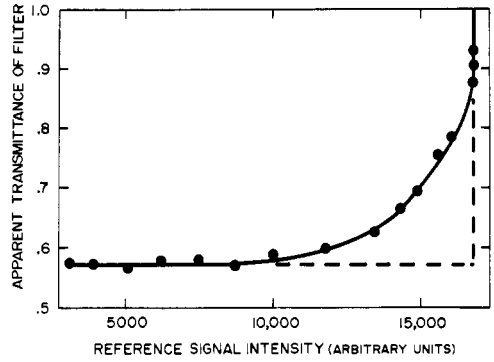

Figure 6. Nonlinearity near detector saturation

ber of photodiodes) that the beam samples in a wavelength channel changes as successive channels are placed closer together. Along the rising portion of the graph, adjacent channels are far enough apart that when the center of the beam travels down the center of one channel, the edges of the beam do not scan any of the adjacent channel. Along the plateau, as the beam center travels down a channel center, the beam edge overlaps a portion of the next adjacent channel. When that next channel is scanned, the effective area is reduced since some of the channel has already been sampled. Across this plateau region, the reduction in effective area and the increase in exposure time balance each other. In the descending region of the graph, the wavelength channels are so close together that the beam completely overlaps more than one channel. As a result, the signal drops rapidly. The intersection of the rising and plateau sections gives the effective width of the beam as about 1/192 of the width of the target face (12.7 mm) or 66 μm. Considering that with the present optical system there are 230 nm within the vidicon detector window, the indicated wavelength resolution is about 1.2 nm for our system, assuming that our hypothesis correctly explains the observations. As a rough check we uniformly illuminated the target and blocked one side with a piece of black tape. If we assumed the tape edge to be perfectly straight and aligned with the scan, the target response at the tape edge indicated a beam width of about 1/55 of the target width, which corresponds to a wavelength resolution of about 4 nm.

These observations indicate that although our system can access up to 4096 electronic channels, in actuality, the number of attainable channels of spectral information is limited to 192 or less. Thus, an 8-bit DAC scanning system would be sufficient to control deflection in the wavelength axis. Since the tube that we used had the photodiodes spaced at 15 μm between centers (*20*), each electronic channel is greater than 4 diodes wide.

Signal Linearity. The signal (I) produced by the silicon vidicon is proportional to the area in a channel (A), the light flux on that channel (N), and the ratio of the times spent exposed to light (T_e) and reading out the signal (T_r) or:

$$I \propto AN(T_e/T_r) \quad (1)$$

In chemical measurements, N is related to the concentration of some species. It is therefore necessary to know the range over which the observed signal varies linearly with N. Combinations of neutral density filters were used to vary N, and the observed intensity at 550 nm was measured. With no filter in the optical path, the gain of the amplifier preceding the ADC was adjusted so that the converter received a full scale 10-volt input when the vidicon target was at about 20% of saturation. (Since some nonlinearity was expected near saturation, another study would concentrate on that region.) The value of the observed signal vs. the transmission of the filters (proportional to the light flux incident on the detector) was measured for filter transmissions from 1.0 to 0.001. When the signal had dropped to 10% and again when it reached 1% of its original value, the gain of the amplifier was increased to make use of more bits in the converter; all data were scaled to the original amplifier gain setting. On a plot of log(response) vs. log(T), the data points fell along a straight line extending over three orders of magnitude with a least squares slope of 0.9906. A t-test indicated that, at the 95% confidence level, the slope of the line was not significantly different from unity. Fitting the response data to a linear equation yielded a linear correlation coefficient of 0.9994. Pardue has reported similar results (*12*).

To study the response near saturation, the amplifier gain was reduced such that the detector saturation occurred at approximately 90% of the converter's full scale. The transmission of a single neutral density filter (T = 0.574) was measured (at 550 nm) as the intensity of the source was varied. The magnitude of the reference signal (with no filter in the path) was used as a measure of source intensity. The results are shown in Figure 6. The dashed line indicates the response for a target that has constant sensitivity to saturation; a constant value would be recorded until the target saturated and then the apparent transmittance would rise to 1.00. The solid line through the experimental points indicates that the sensitivity begins to fall off at about 60% of saturation. Nonlinearity of response occurring this far from saturation was not anticipated, as the observation has not been mentioned in the literature. In all studies performed after this discovery, care was taken to adjust the amplifier to keep measurements within the linear response region.

Noise. Photoelectric detectors exhibit a component of the observed signal which is not related to the properties being measured and which must be subtracted out of the total signal. This component is the dark current or background and is due to thermally created photoelectrons or photocarriers. The dark current is often subtracted rather automatically when the detector is "zeroed". With the vidicon detector, and other imaging devices, this process is not so simple, since each channel has a different dark current level. This dark current is often called "fixed pattern noise" (*8*) since it resembles the hash due to random noise but is not eliminated by signal averaging.

Every time a spectrum is recorded, the dark signal can be recorded (with averaging to reduce random noise) and subtracted. Alternatively, the dark signal can be recorded and stored in the computer or on tape to be subtracted from many spectra over an extended period of time (assuming dark current does not change with time). If the dark current is not subtracted, then signal averaging is of limited utility in S/N enhancement. The lower curve in Figure 7 illustrates the improvement in S/N due to signal averaging but without background subtraction. Hash remaining in

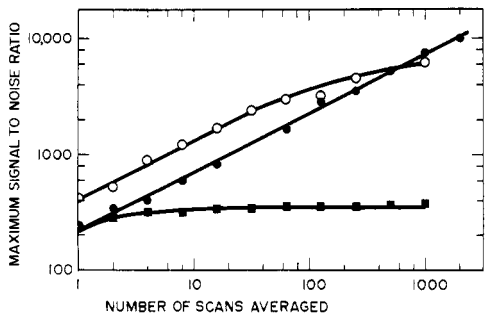

Figure 7. *S/N* enhancement due to signal averaging

the background limits the maximum S/N for this system to 360. (The term "maximum S/N" as used in this paper refers to the ratio of the saturation level output and the root mean square (rms) value of the observed background.) For this study and the following studies concerning noise, the spectra consisted of 128 electronic channels with a scan time of 8 ms per spectrum. The same results were also obtained using spectra with 256 electronic channels.

The random noise component limits the useful dynamic range of the detector. If analysis time permits, signal averaging can be used to eliminate noise from the vidicon spectra. The straight line in Figure 7 displays the improvement in S/N vs. the number of scans averaged. The log–log plot is seen to be linear with a slope of 0.5062. A t-test indicates that, at the 95% confidence level, the slope is not significantly different from ½. So over the range studied, the S/N improves with the square root of the number of scans averaged, indicating that noise on the vidicon's signal is white noise.

The intercept of this line in Figure 7 gives the real-time (or single scan) S/N of the system as 220. This value is approximately the same S/N obtained for a single scan without background subtraction. The system under study is limited mainly by noise in the preamplifier. This means the noise will be random and signal independent (have a constant standard deviation). Low S/N is one of the major limitations of the vidicon spectrometer. Signal averaging has been used to extend the S/N to 10^4 at the expense of the time response (to acquire and average 1024 scans of the sample and 1024 scans of the background of a 128-point spectrum requires 16 s). A different approach can be used to save some time. Rather than acquire a new dark current spectrum, one can store the average of a large number of scans of the dark current and use it repeatedly. The example of S/N enhancement with averaging was repeated using a stored dark spectrum which was the average of 512 scans (upper curve in Figure 7). There are several differences to notice. S/N improvement levels off when the number of sample scans averaged begins to exceed the number of dark scans averaged. Prior to leveling off, S/N improves with the square root of the number of scans averaged. For limited sample averaging, the S/N is enhanced by a factor of $\sqrt{2}$, since the noise is random, over the method of averaging an equal number of scans. Since the total electrical noise on signal (N_S) and on dark current (N_D) scans are independent, the resulting noise, after dark current subtraction, is the rms sum ($N_T = (N_S^2 + N_D^2)^{1/2}$). If the number of dark current scans averaged is much greater than the number of sample scans averaged, then $N_S \gg N_D$ and $N_T \simeq N_S$. If the number of sample scans averaged equals the number of dark current scans averaged, then $N_D = N_S$ and $N_T = N_S\sqrt{2}$.

Target Integration Time. It was desirable to determine the utility of enhancing weak signals by varying the ratio of exposure time to readout time (T_e/T_r). The basic unit of time was taken as one frame (the time to record one spectrum or in this case, 32 ms). To increase T_e and allow signal enhancement due to charge integration on the target, the beam was inhibited from scanning across the target for a number of exposure frames. Then, the scanning circuit was enabled and all the signal that accumulated during the exposure frames was read out during one readout frame.

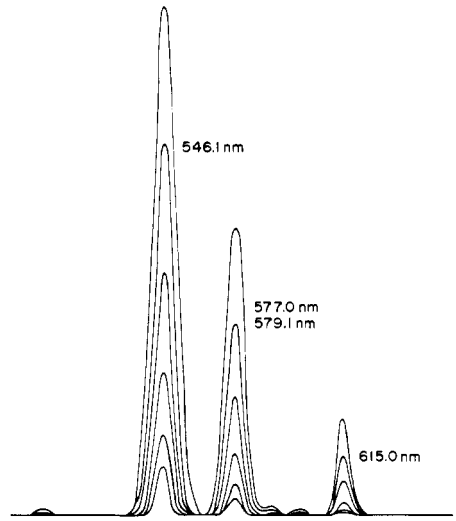

Figure 8. Signal enhancement with charge integration

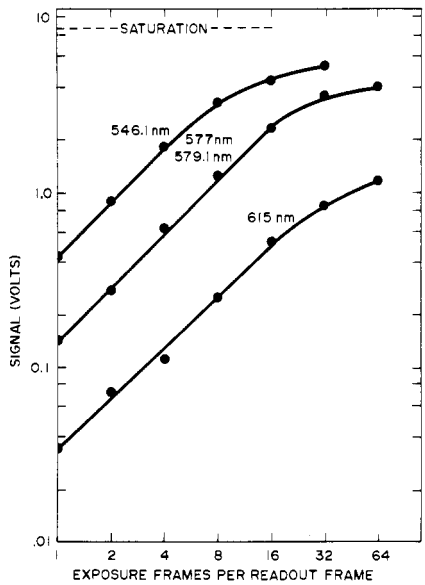

Figure 9. Observed signal vs. exposure time

Figure 8 illustrates superimposed mercury emission spectra recorded for values of T_e/T_r of 1, 2, 4, 8, 16, and 32 exposure frames per readout frame. At long exposure times, weak lines are observed at wavelengths where the signal was originally too low to observe. Intensity vs. integration time for the lines at 546, 615, and the unresolved doublet at 577–579 nm are given in a log–log plot in Figure 9. A t-test indicates that, at the 95% confidence level, the slopes of the linear regions are not significantly different from unity. As the signal approaches saturation or as long integration times are used, nonlinearity occurs. The dark current level at room temperature limited the useful integration time to less than a minute. Peak area vs. T_e/T_r was also measured and was seen to behave as illustrated for line intensity. Unless the accumulated signal approaches saturation, signal intensity increases linearly with integration time up to approximately a 20-fold enhancement.

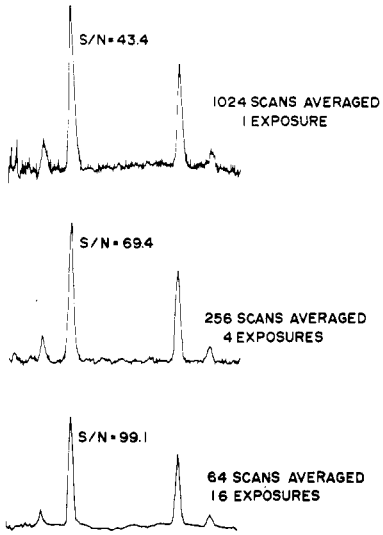

Figure 10. *S/N enhancement with signal averaging and charge integration*

Signal enhancement through charge integration can be used to increase the S/N of a spectrum. In this case, the signal increases linearly with the amount of integration time (until nonlinearity occurs near saturation), while the rms background noise remains constant, increasing only at very long exposure times. So, the S/N increases linearly with the amount of time spent observing the signal rather than with the square root of the time as with averaging. This linear increase in S/N results because the major noise component is independent of the signal level. Figure 10 illustrates three spectra in which the same total amount of time was spent in data acquisition, but the relative times spent on signal averaging and charge integration were varied. Going from the top spectrum to the bottom, a 16-fold larger fraction of the time was spent on charge integration; the S/N of the large peak is seen to increase from 43.4 to 99.1. This observation indicates that, for weak signals, a combination of averaging (to reduce noise) and integration (to enhance signals) may be the optimum procedure. Charge integration enables the detector's dynamic range curve to be shifted to lower intensities by 1–1½ orders of magnitude. The magnitude of the range of the linear region is not increased since the saturation level is also shifted; however integration enables weak signals to be detected. Since all wavelengths are integrated evenly, the technique is of no utility if any intense regions exist in the spectrum. These regions will reach saturation rapidly, and, if integration continues, their signal will spread into adjacent channels (blooming).

Employing target integration with line sources proved to yield a simple, sensitive test for proper orientation of the deflection assembly relative to the spectrum. If the entrance slit and the beam deflection axis are not perfectly aligned, the location of a peak maximum will shift slightly with integration; the extent of the shift increases as target integration time increases and as the slit and deflection axis are further out of alignment.

Random access addressing, although possible with the present system, was not studied, at this time, because of the increased complexity of the required software. Independent of those target areas which one wishes to access, the entire target must be scanned at intervals appropriate to the signal intensity to prevent saturation and blooming. In addition, it is necessary to measure and correct for the unequal integration times of the areas accessed.

The experience with the vidicon spectrometer developed in the course of this research has resulted in our increased appreciation of the strengths and weaknesses of imaging device detectors in analytical spectrometry. This type of detector forms a useful complement to more conventional detectors and is uniquely suited to multicomponent analysis and preliminary investigation of the kinetics of new chemical reactions. We feel that further studies to appreciate the operating characteristics of imaging device spectrometric detectors are necessary to furnish guides for optimum usage. Unique, interactive detection methods deserve particular attention but require instruments under real-time computer control. We have seen that the sensitivity, signal-to-noise ratio, wavelength resolution and scan speed are parameters which may be traded off against one another for optimum performance in a given situation. With a computer-controlled instrument, such as described, these parameters are under software, not hardware, control. During the course of a chemical measurement, these parameters can undergo real-time computer controlled optimization.

LITERATURE CITED

(1) G. Horlick and E. G. Codding, *Appl. Spectrosc.*, **29**, 167 (1975).
(2) K. W. Jackson, J. M. Aldous, and D. G. Mitchell, *Appl. Spectrosc.*, **28**, 569 (1974).
(3) K. M. Aldous, D. G. Mitchell, and K. W. Jackson, *Anal. Chem.*, **47**, 1034 (1975).
(4) K. W. Busch, N. G. Howell, and G. H. Morrison, *Anal. Chem.*, **46**, 2074 (1974).
(5) D. O. Knapp, N. Omenetto, L. P. Hart, F. W. Plankey, and J. D. Winefordner, *Anal. Chim. Acta*, **69**, 455 (1974).
(6) A. Danielsson, P. Lindblom, and E. Söderman, *Chem. Scr.*, **6**, 5 (1974).
(7) D. L. Wood, A. B. Dargis, and D. L. Nash, *Appl. Spectrosc.*, **29**, 310 (1975).
(8) E. G. Codding and G. Horlick, *Spectrosc. Lett.*, **7**, 33 (1974).
(9) T. E. Cook, M. J. Milano, and H. L. Pardue, *Clin. Chem.*, **20**, 1422 (1974).
(10) M. J. Milano and H. L. Pardue, *Anal. Chem.*, **47**, 25 (1975).
(11) G. Horlick and E. G. Codding, *Anal. Chem.*, **46**, 133 (1974).
(12) M. J. Milano, H. L. Pardue, T. E. Cook, R. E. Santini, D. W. Margerum, and J. M. T. Raycheba, *Anal. Chem.*, **46**, 374 (1974).
(13) M. J. Milano and H. L. Pardue, *Clin. Chem.*, **21**, 211 (1975).
(14) G. Horlick, E. G. Codding, and S. T. Leung, *Appl. Spectrosc.*, **29**, 48 (1975).
(15) Y. Talmi, *Anal. Chem.*, **47**, 658A (1975).
(16) Y. Talmi, *Anal. Chem.*, **47**, 697A (1975).
(17) T. A. Nieman, F. J. Holler, and C. G. Enke, *Anal. Chem.* in press.
(18) B. K. Hahn and C. G. Enke, *Anal. Chem.*, **45**, 651A (1973).
(19) G. Davis, *Radio Electron.*, 23 (July 1969).
(20) R. E. Johnson, *Application Note*, **AN-4623**, RCA Electronics Components, 1971.

RECEIVED for review August 8, 1975. Accepted December 8, 1975. One of us (TAN) gratefully acknowledges support from fellowships received from the MSU Chemistry Department, the Eastman Kodak Co., and the Analytical Division of the ACS (sponsored by the Procter and Gamble Co.).